ISSN 2004-2965 Energy Proceedings, Vol. 19, 2021

International Conference on Applied Energy 2021
Nov. 29 - Dec. 5, 2021, Thailand/Virtual
Paper ID: 430

Optimal Operation of Multi-Energy System Integrated with an Alkaline Electrolyzer Dynamic Power-to-Hydrogen&Heat ($P2H^2$) Model

Chunjun Huang[1], Yi Zong[1*], Shi You[1], Chresten Træholt[1]

1 Center for Electric Power and Energy, Technical University of Denmark, Roskilde, 4000, Denmark

ABSTRACT

Apart from producing green hydrogen, the commercial alkaline electrolyzer (AE) could also be a potential heat supply source by recycling the waste heat during the electrolysis process. In this paper, a dynamic power-to-hydrogen&heat ($P2H^2$) model is proposed to characterize the interaction of hydrogen and heat supplying in an AE stack. Based on the presented model, furthermore, a rule-based strategy (RBS) and an operation cost-minimization oriented Mixed Integer Linear Programming (MILP)-based strategy (MILPBS) are developed for enabling the operational flexibility of a multi-energy system (MES) integrated with the $P2H^2$ model. Several cases are studied to show the effectiveness and limitations of the two strategies with comparative performance analysis for different application scenarios.

Keywords: wind power, alkaline electrolyzer, power-to-hydrogen, waste heat recycling, operation optimization

1. INTRODUCTION

Green hydrogen from water electrolysis utilizing renewable power is increasingly expected to facilitate the reduction of CO_2 emission and energy decarbonization [1]. When integrating the electrolyzer into an energy system, many researches currently have focused on exploiting the operational flexibility of electrolyzer modelled as a power-to-hydrogen (P2H) solution, where the optimal planning or scheduling for various distributed energy resources (DERs) installed in a multi-energy system (MES) are extensively investigated. In [2–5], the optimal sizing problems for a stand-alone microgrid or hybrid renewable system integrated with hydrogen energy storage system (HESS) are conducted, where the operating strategy of energy system utilizes a rule-based strategy (RBS) or a cost optimization driven strategy. Besides, the economic operation of DERs are also investigated [6,7] to optimally implement an economic energy management.

Among the various electrolyzers, the alkaline electrolyzer (AE) currently achieves commercial applications [8]. Besides, the AE could be an excellent flexibility source as an energy prosumer through both hydrogen production and recovered heat, performing as both P2H and power-to-heat solution. However, existing researches rarely consider the potential heat supplying capability of electrolyzer, and usually assume a linear model to characterize the relation between its consumed power and hydrogen production.

Motivated by the above considerations, this research develops a dynamic power-to-hydrogen&heat ($P2H^2$) model to characterize the interaction of various energy flows in AE stack. Moreover, the operating performances are investigated when integrating the $P2H^2$ model into an MES, by developing two operating strategies including an RBS and an economical operating strategy.

2. DYNAMIC $P2H^2$ MODEL OF AE

As shown in Fig. 2, the topology of AE mainly consists of an electrolyzer stack combined by several cells and balance of plant (BOP) for enabling the heat-transfer process like a pump and heat exchanger (HE). During the water electrolysis process, the AE will consume the DC electricity to produce hydrogen meanwhile releasing waste heat. Moreover, the AE is linked with a district heating system (DHS) through the HE which supporting the heat exchanging between AE and DHS, thereby enabling the possible flexibility for the DHS operation.

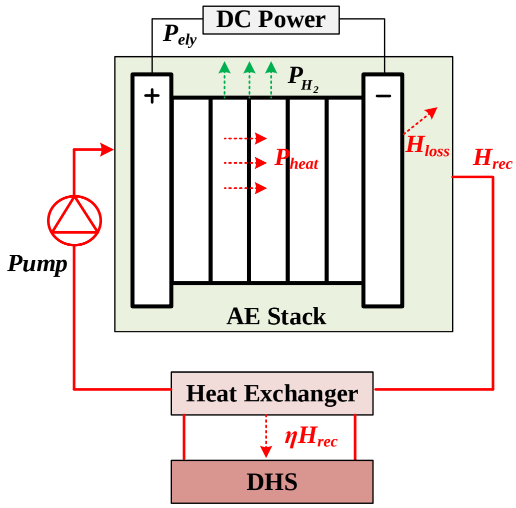

Fig. 1. Basic topology of an AE

2.1 *Electrochemical model*

According to the energy flow shown in Fig. 1, the relation between the consumed power P_{ely} and production of hydrogen and heat can be given as [9]

$$P_{H_2} = \eta_{ely} P_{ely} \tag{1}$$

$$P_{heat} = \left(1 - \eta_{ely}\right) P_{ely} \tag{2}$$

where the electrolysis efficiency η_{ely} depends on the ratio of the cell voltage U_{cell}, and the thermoneutral voltage U_{tn}. Both of them are nonlinear with the stack temperature T_{ely}, which is expressed by

$$U_{cell} = U_{rev} + U_{ohm} + U_{act} = f_1\left(T_{ely}, I_{cell}\right) \tag{3}$$

$$\eta_{ely} = \frac{U_{t_n}}{U_{cell}} = \frac{f_2\left(T_{ely}\right)}{f_1\left(T_{ely}, I_{cell}\right)} = f_3\left(T_{ely}, I_{cell}\right) \tag{4}$$

where the function sets $f_{i=1,2,3}()$ are nonlinear, and the detailed formulation has been given in [10]. The (4) shows the electrolysis efficiency is characterized by a nonlinear function regarding the stack temperature and consumed current or power. Substituting the (4) into (1) and (2), hence the hydrogen and heat power will be nonlinear with the power consumed.

2.2 *Hydrogen production model*

Due to the low operating temperature of AE, the higher heat value (HHV) of hydrogen $Q_{hhv}^{H_2}$ is used to evaluate hydrogen production. The mass level (kg) of hydrogen produced over a given interval is

$$m_{ely}^{H_2} = \frac{\eta_{HHV} P_{ely}}{Q_{hhv}^{H_2}} T_s \approx \frac{P_{H_2}}{Q_{hhv}^{H_2}} T_s \tag{5}$$

where T_s denotes the a given interval between two regulation events, which equals to one hour.

2.3 *Thermal model*

During the heat-transfer process in the AE stack, the temporal stack temperature evolution could be equivalently characterized by a thermal storage model with a lumped capacitance [10], which is formulated by

$$T_{ely}\left(k+1\right) = T_{ely}\left(k\right) + \frac{P_{heat} - H_{loss} - H_{rec}}{C_{ely}} T_s \tag{6}$$

where H_{loss} is the heat loss to the ambient; H_{rec} is the recovered heat; C_{ely} is the overall thermal capacity.

2.4 *Integrated P2H² model*

Combining the previous sub-models (1)~(6), an integrated AE model denoted by P2H² could be obtained as shown in Fig. 2. This model characterizes the interaction of various energy sectors including the electricity, heat and hydrogen sectors. Hence, it is suitable for exploiting the interacted flexibility of AE integrated into an MES. In addition, the nonlinear *U-I* relation of cell and electrolysis efficiency causes the nonlinear pattern of hydrogen production and temperature evolution indicated by (5) and (6) regarding the consumed electricity.

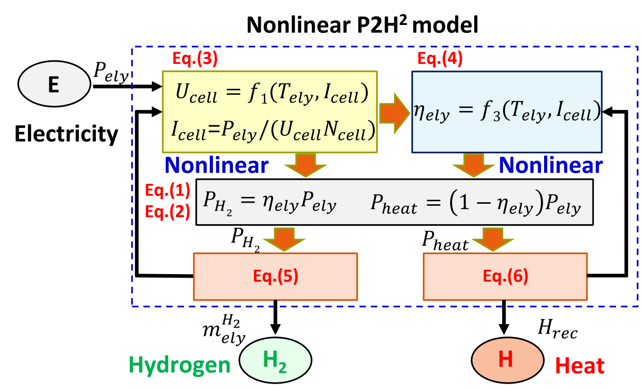

Fig. 2. Schematic of the nonliear P2H² model of AE

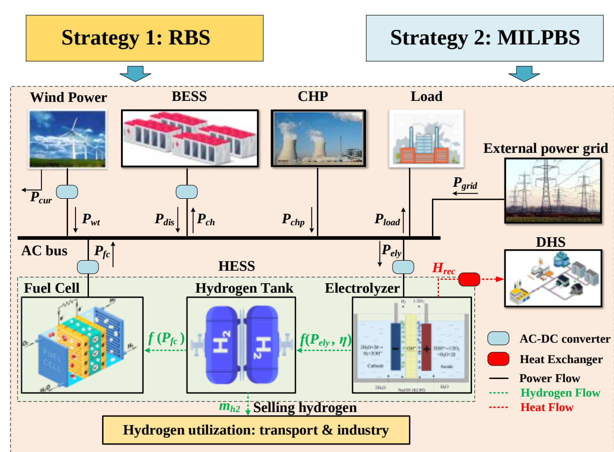

Fig. 3. Topology of an MES ingrated with various DERs

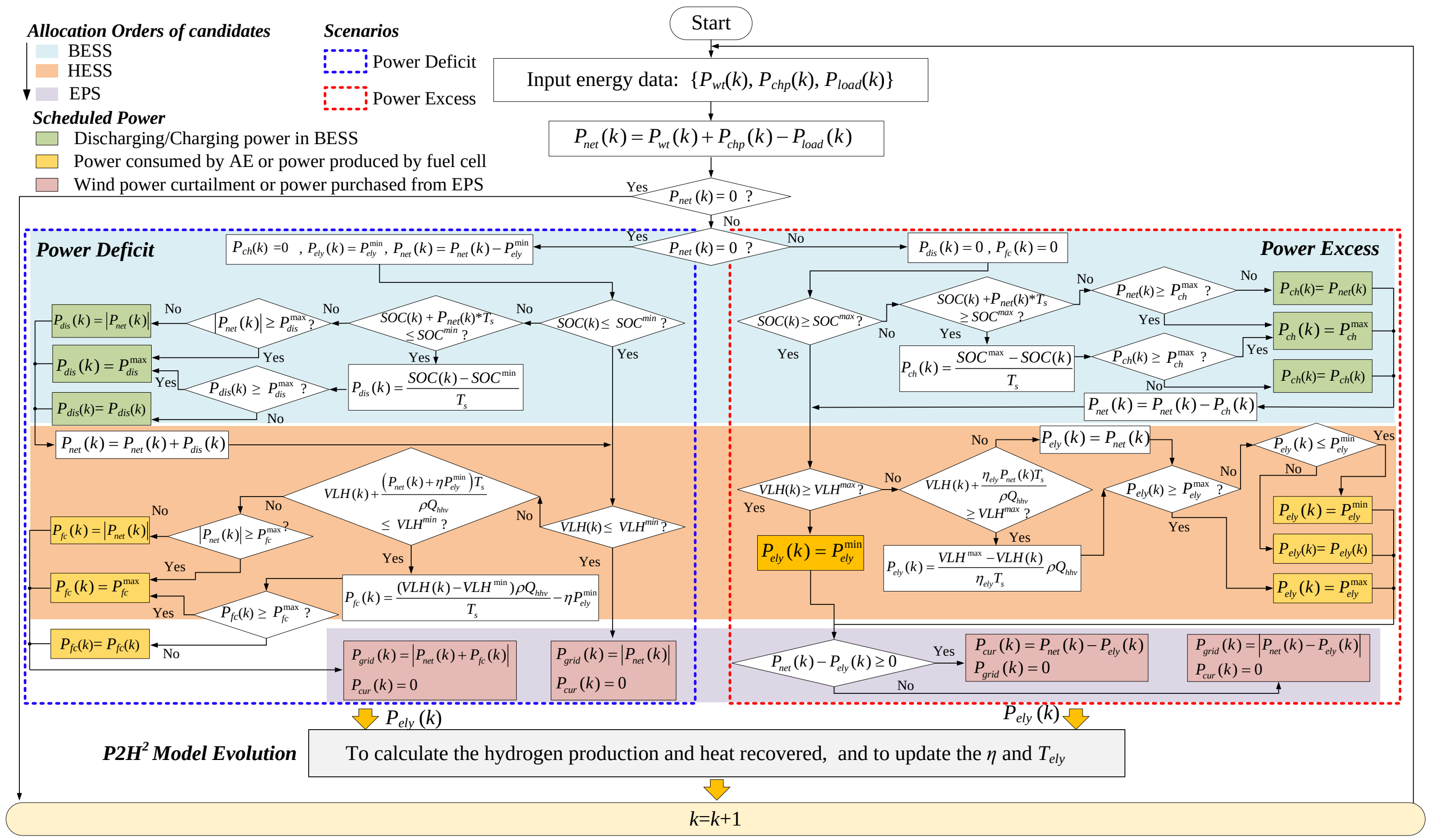

Fig. 4. Control diagram of the rule-based strategy

3. OPERATING STRATEGY FOR MES INTEGEATING WITH THE P2H^2 MODEL

Fig. 3 deficits the topology of an MES integrated with various DERs, which equivalently simulates the Bornholm energy island [11] by utilizing the similar configuration and real historical operating data of the island. The local electricity is mainly produced by wind power and CHP plants, and transferred to the local electrical loads. Besides, two energy storage systems (ESSs) are installed including a battery-ESS (BESS) and a HESS. In addition, the MES is connected to an external electric power system (EPS) and an DHS.

3.1 Rule-based Strategy

Firstly, a rule-based strategy is presented to determine the scheduling of MES, and the control diagram is shown in Fig. 4. The basic principle is to maintain the power balance of MES by allocating the current network power (P_{net}) to three candidates including two ESSs componets and the EPS. The power allocation order is marked by different background colors shown in Fig. 4, where the deployment of P_{net} between the two ESSs follows the rule of BESS prior to HESS, and last to the EPS. The switching of three candidates is determined by checking not only the constraints of the capacity and instantaneous power exchanging (P_{dis} and P_{ch}) for ESSs at time k, but also the limitations of capacity predicted at time k+1. Under the power excess scenario, for instance, the constraints of BESS is firstly checked, including its state of charge (SOC) and charging power P_{ch} at time k, and the predicted SOC at time k+1. After these constraints checking, the final scheduled charging power will be determined as marked by the green box in Fig. 4. Then, the similar constraints of volume level of hydrogen (VLH) and power are evaluated for HESS to obtain the consumed power of the AE shown in the yellow box. Finally, based on the rule of total power balance, the abandoned wind power (P_{cur}) and purchased power from EPS (P_g) are allocated, highlighted by the red box.

After producing the scheduled power P_{ely} for the AE, it is input to the P2H^2 model to obtain the hydrogen production and recovered heat, as well as to update the electrolysis efficiency and stack temperature. Basically, the RBS satisfies the physical constraints of MES involving system stability and the safe margin of DERs, but without seeking an operation cost optimization.

3.2 Cost-minimization oriented MILP-based strategy

To enable the economical operation of MES, another cost- minimization oriented MILP-based strategy

(MILPBS) is developed. The objective function is to minimize the total operation cost (OC) including the variable OC in which the revenues of selling heat and hydrogen produced by AE, and the utilization cost of ESSs are considered. Thus, the objective function can be formulated by

$$\min_{U} J_{sum} = \min_{U}\left(J_{op} + \alpha J_{bess} + \beta J_{hess}\right) \tag{7}$$

$$J_{op} = \sum_{i=1}^{N}\left(\left(C_g^i P_g^i + C_{cur}^i P_{cur}^i - C_{heat}^i H_{rec}^i\right)T_s - C_{H_2}^i m_{H_2}^i\right) \tag{8}$$

$$J_{bess} = \sum_{i=1}^{N}\left(\frac{C_b}{2N_{cycles}}P_{ch}^i + \frac{C_b}{2N_{cycles}}P_{dis}^i\right) \tag{9}$$

$$J_{hess} = \sum_{i=1}^{N}\left(\frac{C_{ely}^{capex}}{N_{ely}^h} + C_{ely}^{OM} + \left(\frac{C_{fc}^{capex}}{N_{fc}^h} + C_{fc}^{OM}\right)\delta_t^{fc}\right)T_s \tag{10}$$

where two weight factors α and β are used to scale-up the utilization costs of BESS and HESS, to make these three cost terms be comparable when formulating the hourly MES operation problem. In addition, the objective function will be constrained by the physical limits of MES operation, which are given as:

1) Power balance

$$P_{wt}^i + P_{chp}^i + P_{dis}^i + P_{fc}^i + P_g^i = P_{ch}^i + P_{ely}^i + P_{cur}^i + P_{load}^i \quad \forall i \in \Omega \tag{11}$$

2) Boundary of power purchased and wind curtailment

$$\delta_g^i P_g^{\min} \le P_g^i \le \delta_g^i P_g^{\max} \quad \forall i \in \Omega \tag{12}$$

$$\left(1-\delta_g^i\right)P_{cur}^{\min} \le P_{cur}^i \le \left(1-\delta_g^i\right)P_{cur}^{\max} \quad \forall i \in \Omega \tag{13}$$

3) Models of BESS

$$SOC(i+1) = SOC(i) + P_{ch}^i T_s - P_{dis}^i T_s \quad \forall i \in \Omega \tag{14}$$

$$SOC^{\min} \le SOC(i) \le SOC^{\max} \quad \forall i \in \Omega \tag{15}$$

$$\delta_b^i P_{dis}^{\min} \le P_{dis}^i \le \delta_b^i P_{dis}^{\max} \quad \forall i \in \Omega \tag{16}$$

$$\left(1-\delta_b^i\right)P_{ch}^{\min} \le P_{ch}^i \le \left(1-\delta_b^i\right)P_{ch}^{\max} \quad \forall i \in \Omega \tag{17}$$

4) Models of HESS integrated with the P2H^2 model

$$VLH(i+1) = VLH(i) + \frac{P_{H_2}^i T_s}{Q_{hhv}^{H_2}} - \frac{P_{fc}^i T_s}{Q_{hhv}^{H_2}} - m_{H_2}^i \quad \forall i \in \Omega \tag{18}$$

$$VLH^{\min} \le VLH(i) \le VLH^{\max} \quad \forall i \in \Omega \tag{19}$$

$$\delta_{fc}^i P_{fc}^{\min} \le P_{fc}^i \le \delta_{fc}^i P_{fc}^{\max} \quad \forall i \in \Omega \tag{20}$$

where all of the variable δ are the binary variables to determine the operating state of DERs. Due to the nonlinearity of P2H^2 model, when directly integrated into the optimization model, the optimization is nonlinear programming even non-convex, which is hard to find globally optimal solutions in a fast way. Thus, the nonlinear P2H^2 model is linearized by assuming a constant electrolysis efficiency of AE, which is reasonable especially in high-power operation. As a result, the dispatch model of P2H^2 model could be

$$\forall i \in \Omega \begin{cases} P_{ely}^{\min} \le P_{ely}^i \le \left(1-\delta_i^{fc}\right)\left(P_{ely}^{\max} - P_{ely}^{\min}\right) + P_{ely}^{\min} \\ Eqs.(1) \sim (6)\ with\ \eta_{ely} = const \end{cases} \tag{21}$$

4. RESULTS AND DISCUSSION

To demonstrate the presented operating strategies, two cases are conducted in the Julia 1.5.3 with JuMP v0.21.6 , including Case 1 integrated with the RBS and Case 2 with the MILPBS. The commercial Gurobi solver is used to solve the MILP optimization. Regarding the input data for the MILP optimization, the historical operating data of Bornholm energy island on June 21, 2018, and the external electricity and heat price are utilized, as shown in Fig. 5. Overall, the wind-rich period occurs from 1:00-6:00 and 15:00-24:00 causing a positive network power (P_{net}), while the deficit of wind energy is happening at 7:00-14:00 leading to a negative P_{net}. Besides, compared to the heat price, the day-ahead electricity price is visibly fluctuating particularly reaching a higher level at 7:00-9:00 while dropping to a lower at 22:00-24:00.

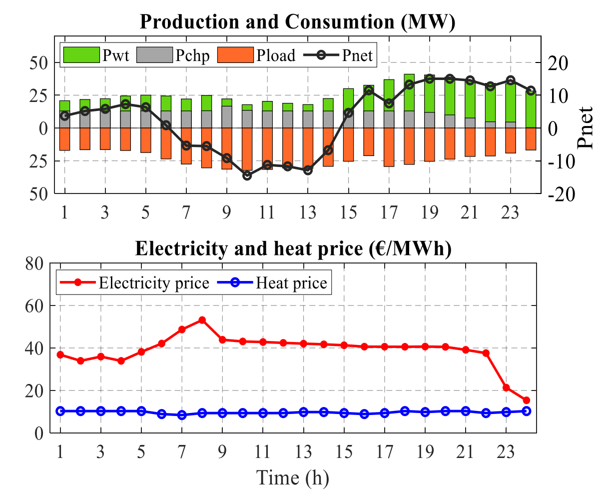

Fig. 5. Historical electricity data of Bornholm island, and energy price on June 21, 2018

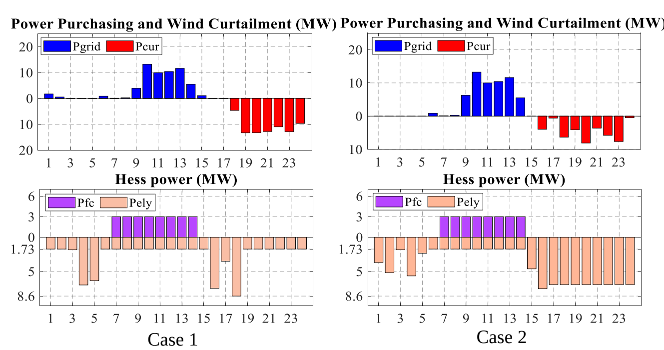

Fig. 6. Scheduled power for various DERs under the two cases

Table 1. Detailed comparison of operation cost under the two cases (€)

Case	Cost_pur	Cost_cur	Cost_H_2	Cost_heat	Cost_op	Cost_bess	Cost_hess	Cost_sum
Case 1	-20.41	18062.56	-1137.57	204.69	17109.27	197.85	2129.11	19436.23
Case 2	-155.55	5377.14	-2777.32	-541.01	1903.27	307.74	2129.11	4340.12

The results of scheduled power for various DERs are shown in Fig. 5. During 7:00-14:00, it shows the two cases have similar behaviors in terms of power production of fuel cell and purchasing power from the external grid. This is because the negative Pnet during these periods would force fuel cell to produce electricity as much as possible and purchase power from the grid to compensate for the lack of local electricity produced. During the wind-rich period at 16:00-24:00, however, Case 2 brings a lower wind curtailment by increasingly consuming more electricity to produce green hydrogen compared to Case 1. This is due to the cost optimization mechanism of Case 2 which optimally drives the electrolyzer to be operating in large-load under the decreasing electricity price conditions.

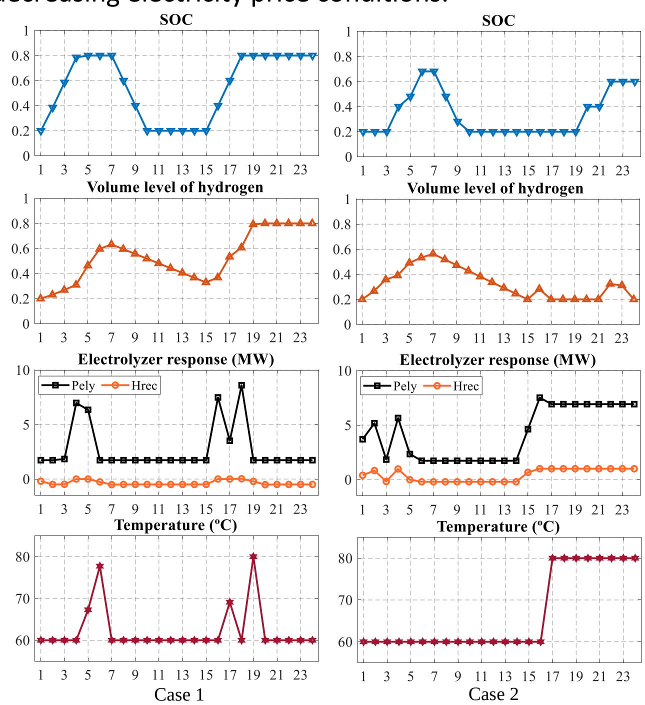

Fig. 7. State response of BESS and HESS under the two cases

Fig. 7 depicts the results of SOC and VLH, which indicates the BESS and HESS rarely reach the maximum storing capacity during wind curtailment in Case 2, thus it can still provide additional down-regulation flexibility for the operation of MES. During 15:00-24:00, because the electrolyzer is operating in large-load in Case 2, much waste heat during the electrolysis process is recycled meanwhile increasing the operating temperature. Conversely, Case 1 rarely recoveries the waste heat but still has heat exchange with DHS by absorbing heat from DHS to maintain the required stack temperature. Thus, it implies the heat flexibility of the electrolyzer could be expected to activate in the two cases due to modelling the thermal dynamic expressed by (6) for the electrolyzer, moreover, Case 2 possibly contributes to earning more profits by selling excess heat to DHS owing to its cost optimization mechanism. As shown in Table 1, Case 2 contributes to a sharp reduction of operational cost to 4340 € from 19436 € in Case 1. This is mainly due to reducing the variable operation cost about 10 times, by optimizing the wind curtailment to avoid much penalty cost, as well as earning additional revenues from selling hydrogen and heat to external industry and DHS.

The results imply the MILPBS is expected to release more flexibility of MES to reduce the wind curtailment and enable a preferable economical operation compared to the RBS. However, the assumption of constant electrolysis efficiency in MILPBS would inevitably cause the deviation of system states to some content. For the scenario, which strictly requires a narrow bandwidth of system state variables , this MILPBS might be not suitable anymore. Conversely, the RBS implements the model evolution thereby effectively mitigating the state error. Besides, the sample structure of RBS enables it could be implemented in a quite fast way, without any optimization calculation. Hence, the RBS would be a preferable candidate for high real-time operating of MES. Therefore, the choice of the two strategies is determined by the application scenario.

5. CONCLUSION

This paper presents a comprehensive $P2H^2$ model of AE to characterize the synergies of hydrogen and heat supplying regarding the consumed electricity. Furthermore, two optimal operating strategies for MES integrated with the $P2H^2$ model, are developed by releasing the operation flexibility itself. The case studies reveal the MILPBS solution can release more operational flexibility, reduce the operation cost and enhance the wind integration, but it might cause a deviation of system states, which could be effectively mitigated in RBS. Hence, the two strategies are suitable for different MES scenario. In the future study, the MILPBS will be improved to reduce the system state deviation while ensuring a preferable economical operation.

ACKNOWLEDGEMENT

This work is supported by "IECC" (No.8087-00019B) and "PRESS" (No. 8073-00026B) projects granted by the Danish Innovation Funding and the Danish Agency for Science & Higher Education, respectively. In addition, the PhD student, Chunjun Huang, is jointly supported by the China Scholarship Council and Technical University of Denmark.

REFERENCE

[1] Kakoulaki G, Kougias I, Taylor N, Dolci F, Moya J, Jäger-Waldau A. Green hydrogen in Europe – A regional assessment: Substituting existing production with electrolysis powered by renewables. Energy Convers Manag 2021;228.

[2] Li B, Roche R, Miraoui A. Microgrid sizing with combined evolutionary algorithm and MILP unit commitment. Appl Energy 2017;188:547–62.

[3] Li B, Roche R, Paire D, Miraoui A. Sizing of a stand-alone microgrid considering electric power, cooling/heating, hydrogen loads and hydrogen storage degradation. Appl Energy 2017;205:1244–59.

[4] Rullo P, Braccia L, Luppi P, Zumoffen D, Feroldi D. Integration of sizing and energy management based on economic predictive control for standalone hybrid renewable energy systems. Renew Energy 2019;140:436–51.

[5] Marocco P, Ferrero D, Lanzini A, Santarelli M. Optimal design of stand-alone solutions based on RES + hydrogen storage feeding off-grid communities. Energy Convers Manag 2021;238:114147.

[6] Garcia-Torres F, Bordons C. Optimal Economical Schedule of Hydrogen-Based Microgrids With Hybrid Storage Using Model Predictive Control. IEEE Trans Ind Electron 2015;62:5195–207.

[7] Cau G, Cocco D, Petrollese M, Knudsen Kær S, Milan C. Energy management strategy based on short-term generation scheduling for a renewable microgrid using a hydrogen storage system. Energy Convers Manag 2014;87:820–31.

[8] Buttler A, Spliethoff H. Current status of water electrolysis for energy storage, grid balancing and sector coupling via power-to-gas and power-to-liquids: A review. Renew Sustain ENERGY Rev 2018;82:2440–54.

[9] Li J, Lin J, Song Y, Xing X, Fu C. Operation Optimization of Power to Hydrogen and Heat (P2HH) in ADN Coordinated With the District Heating Network. IEEE Trans Sustain ENERGY 2019;10:1672–83.

[10] Ulleberg Ø. Modeling of advanced alkaline electrolyzers: A system simulation approach. Int J Hydrogen Energy 2003;28:21–33.

[11] " Bornholm can become the world's first energy island", [Online] Available: https://stateofgreen.com/en/partners/orsted-a-global-leader-within-green-energy/solutions/bornholm-can-become-the-worlds-first-energy-island, 2021.